Reconciling the Okubo-Zweig-Iizuka rule with strong pair creation

Paul Geiger
Department of Physics, University of Toronto, Toronto, Canada M5S 1A7

Nathan Isgur*
Continuous Electron Beam Accelerator Facility, Newport News, Virginia 23606
(Received 26 December 1990)

One of the mysteries of the Okubo-Zweig-Iizuka (OZI) rule is that it is characterized by a scale $\Lambda_{\rm OZI}$ that is small compared to a typical hadronic width Γ, whereas unitarity would lead one to expect $\Lambda_{\rm OZI}\sim\Gamma$. We show that while *individual* virtual decay channels contribute to OZI violation with this expected strength, the coherence between all such channels can conspire to make $\Lambda_{\rm OZI}\ll\Gamma$, as observed.

I. INTRODUCTION

Although it has extensive support from experiment, the origin of the Okubo-Zweig-Iizuka (OZI) rule [1–3] is mysterious. There are, it is true, various limits of QCD in which the observed suppression of the $q\bar{q}$ "hairpin-turn" diagrams characteristic of the rule (see Fig. 1) would be expected. In the heavy-quark limit $Q_1\bar{Q}_1\to Q_2\bar{Q}_2$ mixing is suppressed by α_s^2 and α_s^3, respectively, in the 0^{-+} and 1^{--} ground states and their radial excitations, and is even smaller for orbitally excited states in which annihilation is suppressed by centrifugal-barrier effects. Thus the OZI rule is natural in such a limit. It is also natural in the large-N_c limit where such diagrams are suppressed by $1/N_c$.

It is, however, difficult to associate the observed validity of the OZI rule in light-quark systems with either of these limits for very basic reasons emphasized by Lipkin [4]: OZI-rule violation can always proceed by a *two-step* process involving the *amplitudes* for virtual decay channels [see Fig. 2, corresponding to Fig. 1(b)]. This is the conundrum with which we will be concerned in this paper: since typical OZI-allowed decay widths are observed to have strengths of order $\Lambda_{\rm QCD}$, the real parts of mass matrices (which include OZI-violating off-diagonal terms such as that of Fig. 2) should also be of order $\Lambda_{\rm QCD}$, while experimentally such amplitudes are characterized by a scale $\Lambda_{\rm OZI}\ll\Lambda_{\rm QCD}$. For example, $m_\omega-m_\rho\sim\Lambda_{\rm OZI}\sim 10$ MeV but, as we will see below, virtual decays of the ρ into ground-state mesons ($\pi\pi$, $\pi\omega$, $\eta\rho$, $\eta'\rho$, and $\rho\rho$) alone will produce a ρ mass shift of the order of -1 GeV. Thus although the large-N_c prediction that $\Gamma_\rho/m_\rho\sim 1/N_c$ may be considered successful, and although as $N_c\to\infty$ one might indeed see both a narrow resonance and OZI-rule-respecting world, this does not address the basic puzzle: our world is one in which OZI violations are much smaller than widths, in apparent contradiction to the naive expectation from unitarity depicted in Fig. 2 that $\Lambda_{\rm OZI}$ will have a strength typified by such widths.

The graphs which contribute to meson propagators in QCD can be classified by their topology (see Fig. 3) into OZI conserving and OZI violating. In an earlier paper [5] we showed that although OZI-conserving bubble graphs [the second graph in Fig. 3(a)] have a large magnitude, in a string picture their main effect is to renormalize the string tension. Note that such graphs correspond to virtual-meson loops in which the quark-antiquark pair created in the first decay vertex is annihilated in the second (compare with Fig. 2). Individual intermediate

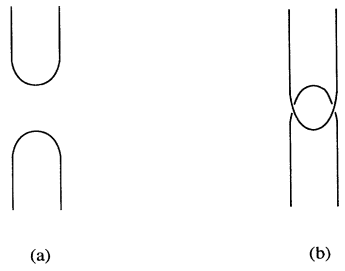

FIG. 1. A diagram associated with OZI-rule violation shown in two time orderings.

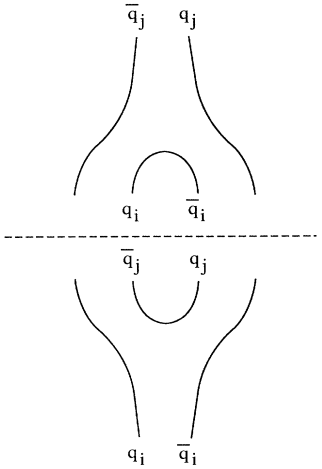

FIG. 2. OZI violation via two OZI-allowed amplitudes.

states in such loops give mass shifts $\Delta m \sim \Gamma$ as expected; only by summing over *all* intermediate states does one see that the bulk of the effect of such processes can be absorbed into a redefinition of the $q\bar{q}$ potential. From the point of view in which one sums over intermediate states, this result is far from obvious. However, from the point of view suggested by Fig. 3(a) one is not so surprised: in the approximation in which one replaces the energy denominators associated with the sum over mesonic intermediate states by a free $q\bar{q}$ energy denominator, the loop acts like a "vacuum polarization" correction to the static quark potential.

In the sum over meson loop graphs, there is of course a second possibility: the quark-antiquark pair created at the first decay vertex may remain as the valence quark and antiquark of the final meson while the second decay vertex annihilates the original $q\bar{q}$ pair. This is the process depicted in Fig. 2 [corresponding to a particular time ordering of Figs. 1 and 3(b)]. As with the bubble graphs of Fig. 3(a), each individual decay channel which can contribute to the total OZI-violating amplitude will give a contribution to $\Lambda_{\rm OZI}$ of order Γ. However, we will see that, as with the OZI-conserving amplitude, it is important to sum over all channels before drawing conclusions on the effects of such processes.

We can easily illustrate how the mechanism we have in mind operates in the context of the flux-tube model for quark pair creation. In this model, a meson decays when the flux tube confining its original quarks breaks, and a new $q\bar{q}$ pair is created with vacuum quantum numbers on the broken flux-tube ends (see Fig. 4). The pair-creation process creates a virtual decay from the original meson to an essentially arbitrary intermediate state and thence to the final meson which produces an OZI-violating amplitude of order Γ. However, if we sum over *all* intermediate states then in the spirit of Fig. 3(a) [i.e., in the closure approximation in which we now neglect the variation of the energy denominators associated with this sum, and the spectator approximation in which we neglect the effect of the pair creation (annihilation) on the original

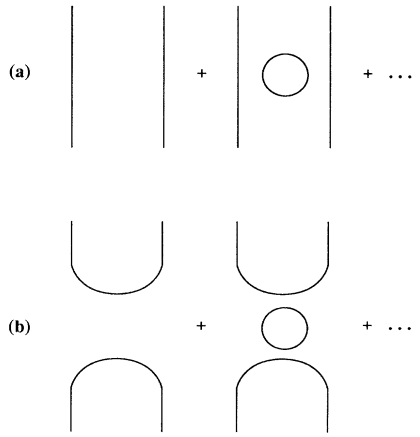

FIG. 3. The two topological classes of graphs contributing to the $\bar{q}_i q_i \to \bar{q}_j q_j$ amplitude corresponding to (a) OZI-conserving and (b) OZI-violating processes; time orderings are, of course, irrelevant for this classification.

FIG. 4. Meson decay by pair creation in the flux-tube-breaking model.

(final) $q\bar{q}$ pair], Fig. 2 would contribute only to the meson propagator with vacuum quantum numbers, *and* OZI *violation in the established meson nonets would vanish.*

In this paper we will examine this mechanism for suppressing $\Lambda_{\rm OZI}$ with respect to Γ in detail, using the ρ-ω-ϕ system as our prototype.

II. PRELIMINARIES

We will, ultimately, directly perform the sum over all intermediate meson states with their appropriate energy denominators and decay amplitudes within the flux-tube model for pair creation mentioned above and using harmonic-oscillator meson wave functions. However, before committing ourselves to such details, we will carefully analyze the structure of the calculation to emphasize that the reduction of $\Lambda_{\rm OZI}$ from its "expected" value Γ is a natural consequence of the above mechanism.

In the SU(3) limit, OZI-violating amplitudes contribute equally to the processes $q_i\bar{q}_i \to q_j\bar{q}_j$ for all i,j ($q_k = u$, d, or s). This conclusion is a consequence of the flavor independence of QCD and the basic topology of the OZI-violating diagrams (see Fig. 3). As a result [6], to lowest order in SU(3)-breaking Δm and in the OZI-violating amplitude A_ω,

$$\Delta m_\rho = 0 \ , \tag{1a}$$

$$\Delta m_\omega = 2A_\omega \ , \tag{1b}$$

$$\Delta m_\phi = \Delta m + A_\omega \ , \tag{1c}$$

$$\phi_\omega = \frac{A_\omega}{\Delta m} \ , \tag{1d}$$

where Δm (assumed here to be large compared to A_ω) is a ϕ-ρ mass difference arising from SU(3) breaking and where ϕ_ω is the deviation of the vector-meson mixing angle from ideal mixing defined by

$$\omega = (\tfrac{1}{2})^{1/2}(u\bar{u} + d\bar{d})\cos\phi_\omega - s\bar{s}\sin\phi_\omega \ , \tag{2a}$$

$$\phi = s\bar{s}\cos\phi_\omega + (\tfrac{1}{2})^{1/2}(u\bar{u} + d\bar{d})\sin\phi_\omega \ . \tag{2b}$$

We see from this general analysis that $m_\omega - m_\rho$ is a measure of OZI violation. [Without the OZI-violating $u\bar{u} \to d\bar{d}$ amplitude, there would be no dynamical rotation of the otherwise degenerate $u\bar{u}$ and $d\bar{d}$ systems into the isospin eigenstates $(\tfrac{1}{2})^{1/2}(u\bar{u} \pm d\bar{d})$.] A survey of the meson nonets gives [7] $A_\omega = +7 \pm 1$ MeV, $A_{f_2} = -22 \pm 3$ MeV, $A_{f_1} = +11 \pm 15$ MeV, $A_{h_1} = -32 \pm 12$ MeV, and $A_{\omega_3} = -12 \pm 4$ MeV from the $\omega - \rho$, $f_2 - a_2$, $f_1 - a_1$, $h_1 - b_1$, and ω_3-ρ_3 mass differences. [We exclude the pseudoscalar mesons from this survey since $\eta - \eta'$ mix-

ing, which arises from the U(1) anomaly, has a special status. In any event, the puzzle we are addressing is how *any* nonet can have $A \ll \Gamma$.] From this list we can see that OZI-violating amplitudes are, as stated in the introduction, typically an order of magnitude smaller than meson widths. Moreover, we see that while A_ω is probably the smallest of these amplitudes, the ρ-ω-ϕ system can serve as a reasonable prototype for our discussion of OZI violation.

The puzzle of the OZI rule is an old one which has been discussed often. There have, in particular, been many discussions [4, 6, 8–10] of the "annihilation diagrams" of Fig. 3(b). Some of these discussions have been perturbative (in which case they include both of the time orderings of Fig. 1), others have considered the contributions of virtual glueballs [in which case they are focusing on the time ordering of Fig. 1(a)], while others, as we do here, concentrated on the unitarity puzzle associated with the virtual decay channels of the time ordering of Fig. 1(b), i.e., Fig. 2.

In this last class of papers are those we have already mentioned by Lipkin [4] in which many of the essential ingredients of the picture of the OZI rule which we propose here were foreshadowed. In particular, Lipkin stressed the importance to the OZI rule of cancellations between different intermediate states and argued that its validity must ultimately involve cancellations not only between states of a given flavor or flavor-spin multiplet, but also between states of different generalized G parity. He also explicitly recognized that the closure and spectator approximations could be important to understanding these cancellations. The reader will see below that our solution to the OZI puzzle has all of the characteristics which Lipkin anticipated. The role of cancellations in the OZI rule (as well as in the analogous suppression of exotic exchanges) was also noted by Schmid, Webber, and Sorensen and by Berger and Sorensen [4]. They pointed out within the context of Regge theory that the cancellations between exchange-degenerate trajectories of opposite G parity occurred naturally and could be arranged to preserve the OZI rule.

Another study which has strong connections to ours is that of Tornqvist (see Ref. [10]). In a series of papers working within the context of the $^3P_0$ model, he has studied the effects of quark loops on the quark model. Since these calculations are restricted to the ground-state channels, they reflect the "higher-order paradox" explicitly. Although he was able to solve the ω-ρ splitting problem thereby encountered by fine-tuning parameters, no general solution was found.

A. The closure limit

The amplitude for the "virtual decay" piece of the OZI-violating process $q_i\bar{q}_i \to q_j\bar{q}_j$ for $q_i \neq q_j$ (i.e., the amplitude for Fig. 2) is

$$A(E) = \sum_n \frac{\langle q_j\bar{q}_j | H_{\rm PC}^{q_i\bar{q}_i} | n \rangle \langle n | H_{\rm PC}^{q_j\bar{q}_j} | q_i\bar{q}_i \rangle}{E - E_n} , \tag{3}$$

where $H_{\rm PC}^{f\bar{f}}$ is the quark-pair-creation operator for flavor f and the set $\{|n\rangle\}$ is a complete set of two-meson intermediate states. As indicated in the Introduction, in the limit that the energy denominators in this expression vary negligibly with n, the sum collapses to a closure relation, giving

$$\begin{aligned} A \propto B &\equiv \sum_n \langle q_j\bar{q}_j | H_{\rm PC}^{q_i\bar{q}_i} | n \rangle \langle n | H_{\rm PC}^{q_j\bar{q}_j} | q_i\bar{q}_i \rangle \\ &= \langle q_j\bar{q}_j | H_{\rm PC}^{q_i\bar{q}_i} H_{\rm PC}^{q_j\bar{q}_j} | q_i\bar{q}_i \rangle . \end{aligned} \tag{4}$$

Thus, if $H_{\rm PC}$ cannot create and destroy pairs with the quantum numbers of $|q_i\bar{q}_i\rangle$ and $|q_j\bar{q}_j\rangle$, A will vanish in the spectator approximation. In the $^3P_0$ model, which we will describe (and advocate) in the following subsection, hadron decays proceed via the creation of a quark-antiquark pair with vacuum quantum numbers only. This model thus predicts in the closure and spectator approximations that virtual decays make no contribution to OZI violation in the established nonets. (It also predicts that OZI violation in the predicted but not yet established scalar-meson nonet will be unique; see below.)

In the next section we will describe the $^3P_0$ model, focusing on the particular version of it that we have used to compute the matrix elements in the numerator of Eq. (3). We will then display the individual terms contributing to the zero expected in the closure approximation (4) for the case of $u\bar{u} \leftrightarrow d\bar{d}$ mixing in the ground state $J^{\rm PC} = 1^{--}$ mesons. Examination of these terms will reveal that the closure sum is driven towards zero by several types of systematic cancellations which, as we will see below, are not badly spoiled when the energy denominators are restored.

B. The $^3P_0$ model

The $^3P_0$ model [11] is a phenomenologically successful quark-pair-creation model for describing strong hadronic decays. It assumes such decays proceed by rearrangement of the quarks in the original hadron with a quark-antiquark pair that is created out of the vacuum in a $^3P_0$ state. In the original formulation of the model, the pair creation was assumed to be pointlike and to occur with equal amplitude everywhere in space. This leads, in the rest frame of A, to the $A \to BC$ meson decay amplitude

$$M(A \to BC) = (2\pi)^{3/2}\gamma_0\phi\Sigma\cdot\int d^3k\,\Phi_B^*(\mathbf{k})\Phi_C^*(\mathbf{k})(2\mathbf{k}+\mathbf{q})\Phi_A(\mathbf{k}-\mathbf{q}/2) , \tag{5}$$

where the Φ's are momentum-space wave functions, $\mathbf{q}$ is the momentum of B, ϕ is a flavor overlap, Σ is a spin overlap, and γ_0, the intrinsic pair-creation strength, is the only parameter of the model. In this model the original q and $\bar{q}$ are

perfect spectators; i.e., their state is unaffected by the pair creation.

A modified version of this model, and a firmer theoretical foundation for it, emerge in the context of a flux-tube picture of hadrons [12,13]. The main new effect in this picture is that the pair is created in a localized region near the original $q\bar{q}$ axis controlled by the overlap of the two new flux-tube wave functions with the old flux-tube wave function (see Fig. 4). With this modification, (5) becomes

$$M=\frac{\gamma_0\phi\Sigma}{(2\pi)^{3/2}}\cdot\int d^3k\, d^3p\, d^3p'\Psi(\mathbf{p},\mathbf{p}')\Phi_B^*(\mathbf{k}+\mathbf{p}'/2)\Phi_C^*(\mathbf{k}-\mathbf{p}'/2)(2\mathbf{k}+\mathbf{q})\Phi_A(\mathbf{k}-\mathbf{q}/2-\mathbf{p})\ , \tag{6}$$

where $\Psi(\mathbf{p},\mathbf{p}')$ is the Fourier transform, with respect to the spatial coordinates $\mathbf{r}$ and $\mathbf{w}$ shown in Fig. 5, of the flux-tube overlap function. (In Ref. 13, this function was taken to have "cigar-shaped" contours, i.e., to fall off exponentially with the perpendicular distance between the created pair and the line joining the original quark and antiquark. We will, to make our calculations tractable, take the function to have spherical contours instead. The implications of this simplification will be discussed below.)

The extensive analysis performed in Ref. 13 showed that this model is quite successful: it fits the approximately 60 measured strong meson decay amplitudes with a mean error of about 25%. Interestingly, the inclusion of the flux-tube overlap function was unimportant to this success, as the finite size of the meson wave functions in (5) already effectively restricted pair creation to small distances from the initial meson. However, since our calculation involves a sum over *all possible* intermediate mesons, the spatial cutoff is at least a calculational necessity. Without it Eq. (3) would create and annihilate pairs with equal strength over all space and the sum would be indeterminate, behaving like infinity minus infinity.

In Ref. 5, we further modified the $^3P_0$ model to include a form factor for the created quark and antiquark: the pointlike $^3P_0$ pair-creation operator, which takes the form $q^\dagger(\mathbf{r})\boldsymbol{\alpha}\cdot\nabla q(\mathbf{r})$ in position space (the α's are Dirac matrices), was replaced by

$$\int d^3u\ \rho(u)q^\dagger(\mathbf{r}+\mathbf{u}/2)\boldsymbol{\alpha}\cdot\nabla q(\mathbf{r}-\mathbf{u}/2)\ , \tag{7}$$

where $\rho(u)=(3/8\pi r_q^2)^{3/2}\exp(-3u^2/8r_q^2)$. This operator creates a $^3P_0$ pair with a mean separation of order the "constituent quark size," r_q. This introduces a new parameter into the $^3P_0$ model but, like the flux-tube overlap function, it is both physically motivated and necessary in order to obtain a finite result when one sums over a complete set of virtual decay channels. (The pointlike version of the pair-creation operator produces an infinite string tension renormalization, as one would expect. In the Appendix, we will describe our method of determining r_q and the sensitivity of our results to changes in r_q.) With the quark form factor in place, we have finally

$$M(A\to BC)=\frac{2}{(2\pi)^{3/2}}\gamma_0\phi\Sigma\cdot\int d^3k\, d^3p\, d^3p'\Psi(\mathbf{p},\mathbf{p}')$$
$$\times\Phi_B^*(\mathbf{k}+\mathbf{p}'/2)\Phi_C^*(\mathbf{k}-\mathbf{p}'/2)(\mathbf{k}+\mathbf{q}/2)\exp\left[-\frac{2r_q^2}{3}(\mathbf{k}+\mathbf{q}/2)^2\right]\Phi_A(\mathbf{k}-\mathbf{q}/2-\mathbf{p}). \tag{8}$$

It is this twice-modified $^3P_0$ formula which we will use to perform the calculations discussed in the following subsection.

C. Evaluation of the closure sum in the vector sector

Let us now examine in detail the closure approximation for the ground-state vector $u\bar{u}$ meson mixing with the corresponding $d\bar{d}$ meson. Recall from Eq. (1) that the ω-ρ mass splitting receives a contribution that is directly proportional to the amount of such mixing. Understanding how the mixing vanishes in the closure approximation is the first step in understanding how m_ω-m_ρ can be small in the full calculation that includes energy denominators.

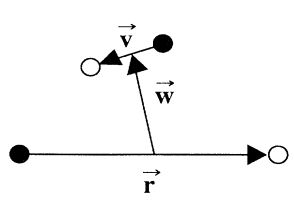

FIG. 5. Position-space coordinates for meson decay by pair creation.

The general term in the closure sum is

$$\langle d\bar{d}|H_{\rm PC}^{u\bar{u}}|n\rangle\langle n|H_{\rm PC}^{d\bar{d}}|u\bar{u}\rangle\ , \tag{9}$$

where n stands for a complete set of quantum numbers for the intermediate states, which we will take to be $\{n_B,l_B,m_{l_B},s_B,m_{s_B};n_C,l_C,m_{l_C},s_C,m_{s_C};q,l,$ and $m\}$, i.e., the radial, orbital, and spin quantum numbers of the intermediate mesons B and C, as well as the (magnitude of the) momentum and the angular momentum of their relative coordinate. We analytically sum over m_{l_B}, m_{l_C}, m, and the quark spins, leaving us with terms that are functions of q labeled by n_B, n_C, l_B, l_C, and l. We display these functions in Fig. 6, ordered by $L\equiv l_B+l_C+l$ and $N\equiv n_B+n_C-2$ (our convention is that the ground state of every l has $n=1$, so the sums start with $N=0$). The

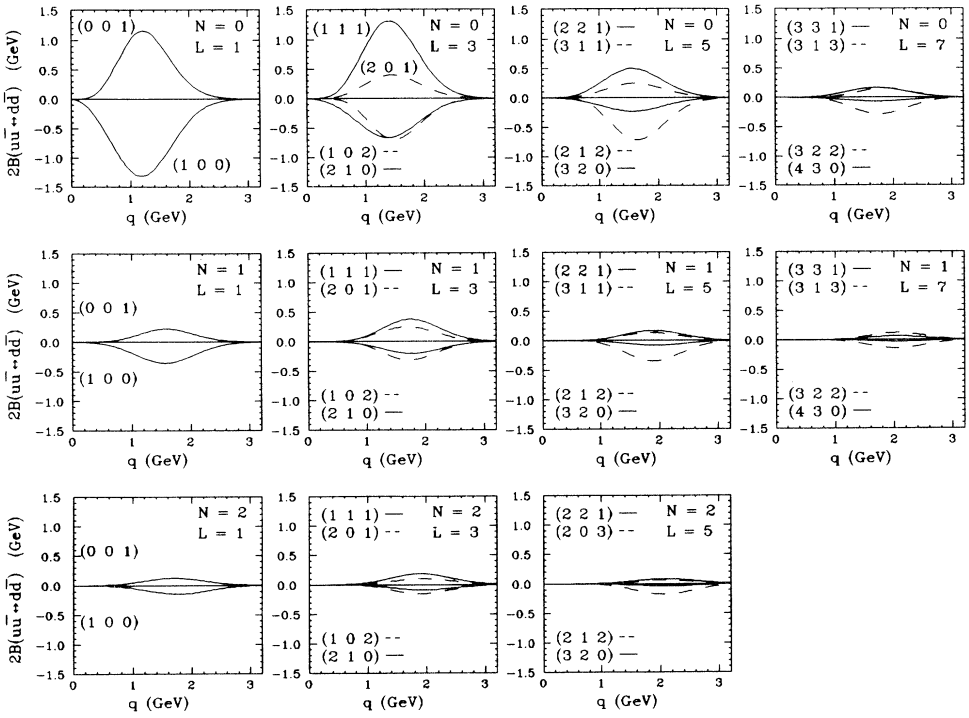

FIG. 6. The terms in the closure sum for B in Eq. (4) ordered by $L \equiv l_B + l_C + l$ and $N \equiv n_B + n_C - 2$, calculated using our canonical parameters $\beta = 0.4$ GeV, $b = 0.18$ GeV^2, and $r_q = 0.15$ fm. The curves are labeled by (l_B, l_C, l); when $l_B \neq l_C$, (l_B, l_C, l) is an abbreviation for $(l_B, l_C, l) + (l_C, l_B, l)$. To avoid overcrowding on the graphs with $L \geq 5$, we show only the "leading" terms, i.e., the $(\kappa, \kappa, 1)$ and $(\kappa+1, \kappa, 0)$ ones and the two largest remaining terms.

graphs were obtained by inserting harmonic-oscillator wave functions into Eq. (8). The oscillator parameter β, defined by $\Phi(\mathbf{k}) \sim$ (polynomial) $\exp(-k^2/2\beta^2)$, was taken to be 0.4 GeV as in Ref. [13], r_q was taken to be 0.15 fm as described in the Appendix, and the flux-tube overlap function was taken to be $\tilde{\Psi}(\mathbf{r}, \mathbf{w}) = \exp(-bw^2/2)$, where $b = 0.18$ GeV^2 is the string tension [13]; this gives $\Psi(\mathbf{p}, \mathbf{p}') = \delta^3(\mathbf{p})(2\pi/b)^{3/2} \exp(-p'^2/2b)$. We emphasize that the closure sum must be zero independent of the parameters β, r_q, and b, so we postpone a discussion of them to the Appendix, where their effect on our calculation of the actual $\omega - \rho$ mass difference will be estimated. The choice of $\tilde{\Psi}(\mathbf{r}, \mathbf{w})$ *is* significant; since it is independent of $\mathbf{r}$, it (like the naive $^3P_0$ model) leads to a spectator approximation for the internal degrees of freedom of the initial $q\bar{q}$ pair. However, the use of this function to simplify our calculation is not misleading in the case at hand. Consider, first of all, a case where $\tilde{\Psi}$ depends on the magnitude of $\mathbf{r}$. Then the angular momentum of the original $q\bar{q}$ pair would still be unaffected by the pair creation, and the closure sum would still give zero for all but $^3P_0$ mesons. Now consider a more realistic, cigar-shaped $\tilde{\Psi}$. The $\mathbf{r}$ dependence of such a function is such that it can change the J^P of the initial $q\bar{q}$ pair, but it can do so only by the addition of $L^{\Pi} = 0^+, 2^+, 4^+, \ldots$. Hence the closure sum will still give zero for the $^3S_1$ ρ-ω-ϕ system.

We now make several observations concerning the graphs of Fig. 6, and comment on them subsequently.

(i) The closure sum does indeed converge towards zero, as illustrated in Table I, where we show the sequence of partial sums. Moreover, the convergence is apparent for quite small values of N and L. (Note that since the $q\bar{q}$ pair is created with one unit of orbital angular momentum on the S-wave ρ and ω wave functions, the three orbital angular momenta l_B, l_C, and l are restricted by the requirement that it be possible to sum them to total angular momentum one.)

(ii) The first two terms in the sum, the nonradially excited terms with $(l_B, l_C, l) = (0,0,1)$ and $(1,0,0) + (0,1,0)$ are very large, but they cancel each other to a very large extent.

TABLE I. (a) An illustration of the rapid convergence of the closure sum. The entries show the integrals of the corresponding graphs in Fig. 6 in units of $\gamma_0^2 \beta^2 / 6\pi^2$. (b) The sequence of partial sums for (a).

(a)

	$L=1$	$L=3$	$L=5$	$L=7$	$L=9$	$L=11$
$N=0$	−184.3	193.6	−4.8	15.3	−0.1	0.9
$N=1$	−93.2	70.3	−15.7	9.7	−1.5	0.8
$N=2$	−18.4	30.4	−8.1	5.2	−1.0	0.5
$N=3$	−9.6	10.6	−3.3	2.3	−0.5	0.3
$N=4$	−2.9	4.0	−1.3	0.9	−0.2	0.1
$N=5$	−1.3	1.5	−0.5	0.3	−0.1	0.0

(b)

	1×1	2×2	3×3	4×4	5×5	6×6
Partial sum	−184.3	−13.6	−30.2	−0.1	−2.8	0.0

(iii) There is a hierarchy of sizes in the remaining terms: the terms with $l=0$ or 1 tend to be larger than the others, and the terms decrease in size uniformly as the excitation numbers increase. Within each stage of the hierarchy, the terms tend to cancel.

(iv) A particular feature of this local cancellation will help it to persist when energy denominators are reinserted. Consider, for example, the large canceling $N=0$, (0,0,1) and (1,0,0)+(0,1,0) terms. The energy denominator of the latter will, at a given q, be larger than that of the former because one of its mesons contains an extra unit of internal orbital angular momentum. However, the P-wave (0,0,1) decay matrix element, with its angular momentum barrier factor q^l, starts off more slowly and peaks later as a function of q than does the S-wave (1,0,0)+(0,1,0) term, tending to compensate for the difference in the energy denominators. We will elaborate upon and be able to quantify this observation below.

Observations (ii) and (iii) can be understood in terms of a peculiar limit. To extract this limit, we explicitly write out the expression for (9), using oscillator wave functions in (8), obtaining

$$\int d^3u\, d^3v\, d\Omega_q e^{-(\mathbf{u}-\mathbf{v})^2/2b}\tilde{\Phi}^*_B(\mathbf{u})e^{-u^2/2\beta^2}\tilde{\Phi}^*_C(\mathbf{v})e^{-v^2/2\beta^2}(\mathbf{u}+\mathbf{v}+\mathbf{q})e^{-r_q^2(\mathbf{u}+\mathbf{v}+\mathbf{q})^2/6}e^{-(\mathbf{u}+\mathbf{v}-\mathbf{q})^2/8\beta^2}Y^*_{lm}(\Omega_q)\ , \tag{10}$$

where the $\tilde{\Phi}$'s are oscillator wave functions, modulo their exponential factors which we have shown explicitly. The cross terms in the exponentials may be rearranged to

$$e^{[\lambda/(1-\lambda)]\mathbf{u}\cdot\mathbf{v}/\beta^2}e^{-\gamma(\mathbf{u}+\mathbf{v})\cdot\mathbf{q}/\beta^2}\ ,$$

where $\lambda/(1-\lambda)\equiv(\beta^2/b-\beta^2r_q^2/3-1/4)$ and $\gamma\equiv(\beta^2r_q^2/3-1/4)$. For the "magic" case $\lambda=\gamma=0$ (corresponding to $r_q=\sqrt{3}/2\beta$ and $b=2\beta^2$), the integrals in (10) simplify, and only states with $e_B+e_C+l=1$ survive. ($e_i+3/2$ is the energy of oscillator i in units of $\hbar\omega$.) In a basis of "spherical" oscillators, this condition is equivalent to $2N+L=1$, so that only the radial ground state, $(l_B,l_C,l)=(1,0,0)$, (0,1,0), and (0,0,1) terms are nonzero. The entire closure cancellation therefore occurs in the analog of the $N=0$, $L=1$ graph of Fig. 6.

We next examine parameters which are close to the magic limit. For $\gamma=0$, consider the expansion

$$(1-\lambda)^{-1/2}e^{-[\lambda/(1-\lambda)](u-v)^2/\beta^2}=\sum_\kappa\lambda^\kappa\frac{(-1)^\kappa}{4^\kappa\kappa!}H_{2\kappa}\left[\frac{u-v}{\beta}\right] \tag{11}$$

for the λ exponential, where $H_{2\kappa}$ is a Hermite polynomial. Inserting this into Eq. (10) and performing the integrations in a basis of "rectangular" oscillators, one easily sees that only $l=0$ and $l=1$ terms survive, and that only those states with energy $e_B+e_C=2\kappa+1-l$ contribute to the $O(\lambda^\kappa)$ term. In the spherical basis, this condition is $2N+L=2\kappa+1$. Since the closure sum vanishes for any λ, it follows that *there is an exact cancellation within each subset of terms corresponding to a given value of* $2N+L$ (for $\gamma=0$). Note that the terms in each such subset will all have similar energy denominators [especially in light of the argument given in point (iv) above], so that there will be a strong tendency for these cancellations to be maintained when the energy denominators are restored.

An expansion in γ also reveals useful information. By substituting

$$e^{-\gamma(\mathbf{u}+\mathbf{v})\cdot\mathbf{q}/\beta^2}=4\pi\sum_{l',m'}i^{l'}jl'(i\gamma q|\mathbf{u}+\mathbf{v}|/\beta^2)\times Y^*_{l'm'}(\Omega_q)Y_{l'm'}(\Omega_{u+v}) \tag{12}$$

into (10) and noting the $j_{l'}(i\gamma q|\mathbf{u}+\mathbf{v}|/\beta^2)\sim\gamma^{l'}$ for small γ, one easily finds that the terms in the closure sum decrease with l: $l=0$ and $l=1$ terms are of order unity, while $l>1$ terms are of order γ^{l-1}.

The "magic" limit is thus somewhat more than an analytic toy. In a light-quark system we expect that the parameters $b^{1/2}$, β, and r_q^{-1} will all be of order $\Lambda_{\rm QCD}$, and their "magic" ratios are consistent with this loose requirement. However, the "magic" ratios are also reasonably close to the phenomenological best values discussed in the Appendix. As a result, the physical closure sum zeros in a very rapid and orderly fashion: as is evident from comparing Figs. 6 and 7, it is sufficiently close to the "magic" closure sum to still have the same structure.

III. CALCULATION OF $m_\omega-m_\rho$

We now proceed to the full calculation of the ω-ρ mass difference arising from virtual decay diagrams. As indicated in Sec. II, this difference is

$$\Delta m_\omega-\Delta m_\rho=2A_\omega\ , \tag{13}$$

where

$$A_\omega=\sum_n\frac{\langle d\bar{d}|H^{u\bar{u}}_{\rm PC}|n\rangle\langle n|H^{d\bar{d}}_{\rm PC}|u\bar{u}\rangle}{M-E_n} \tag{14}$$

with M the common mass of ρ and ω in the absence of OZI violation. To evaluate this sum we used for the numerators the functions displayed in Fig. 6; in the denominators we used the masses calculated in the quark model of Ref. [14] (or in some cases of high n or l, masses extrapolated from those tabulated in Ref. [14]; see Ref. [15]. Our explicit formula for A_ω is

$$A_\omega=\frac{1}{6\pi^2}\sum_{B,C,l,s}\left[\frac{\tilde{M}_A\tilde{M}_B\tilde{M}_C}{M_A}\right]\times\int\frac{dq\,q^2}{E_BE_C}\frac{|M_{ls}|^2}{M-(E_B+E_C)}\ , \tag{15}$$

where B,C are the quantum numbers of the intermediate mesons B and C, the $\tilde{M}$'s are normalization factors discussed in Ref. [13], and the LS amplitude $M_{ls}(q)$ is obtained by applying the Jacob-Wick formula to the helicity amplitudes provided by (8) (see, e.g., Ref. [13]).

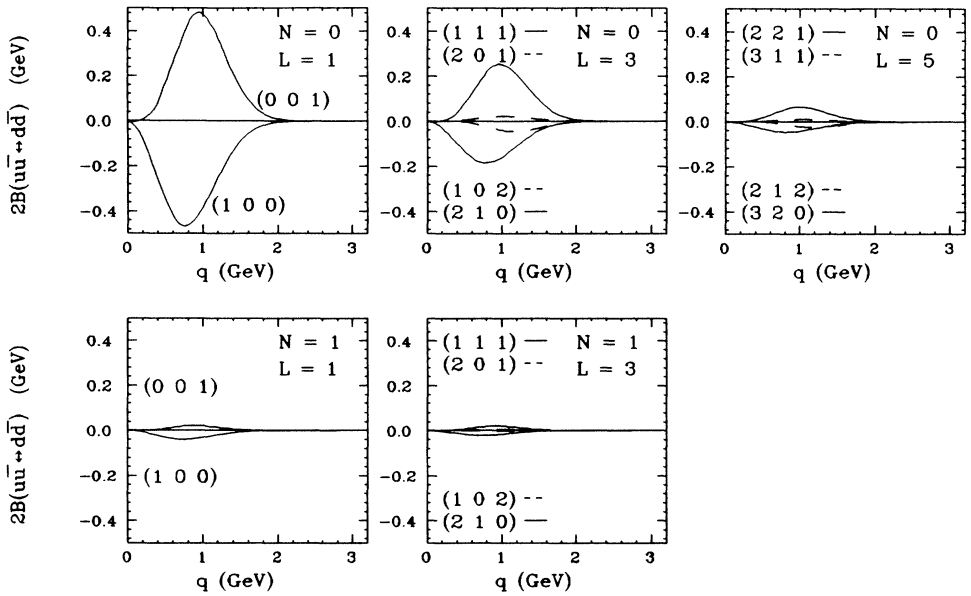

FIG. 7. Legend as for Fig. 6, except that here the parameters $\beta=0.4$ GeV, $b=0.10$ GeV^2, and $r_q=0.30$ fm have been chosen to be close to the "magic" ratios discussed in the text. The structure expected in the vicinity of the "magic" limit is clearly exhibited.

Our results are shown in Table II. In addition, Table III shows the individual mass shifts of ω and ρ from some of their low-lying virtual decay channels. [Notice that Δm_ρ arises entirely from the processes of Fig. 3(a) and corresponds to the "string tension renormalization" mentioned in the Introduction and discussed in Ref. [5]. The processes of Fig. 2 produce an additional shift in m_ω which is that shown in Table II. For example, the +141-MeV contribution of the (0,0,1) term to $\Delta m_\omega - \Delta m_\rho$ may be obtained by comparing the ω and ρ shifts from virtual decays to the ground-state pseudoscalar and vector mesons shown in the top half of Table III. This net shift is one of the two canceling $N=0$, $L=1$ terms analogous to those shown in Fig. 6, and the beginning of a sum of such canceling terms.] We omit from Table III the contributions from strange pairs like $K\bar{K}$ and $K\bar{K}^*$ since channel by channel they produce equal mass shifts in the ρ and ω. The large differential shifts of Table III, together with the disparity in the available channels, re-emphasize the need for a mechanism such as the closure limit to explain the near-perfect cancellation of $\Delta m_\omega - \Delta m_\rho$. These large cancellations also point out the difficulty in any attempt to *accurately* calculate $m_\omega - m_\rho$. The result of our calculation is that the virtual decay channels contribute +13 MeV to this splitting, but this agreement with the measured value is accidental; for reasonable variations in our model parameters it varies by tens of MeV's. The value of this calculation is not to be measured in such terms, but rather in its showing how the scale of $\Lambda_{\rm OZI}$ is naturally reduced from a mass of order $\Lambda_{\rm QCD}$ (see Table III) to a mass of the order of 10 MeV which typifies $\Lambda_{\rm OZI}$ experimentally. We should also emphasize that even if this calculation were accurate, it should not give the experimentally observed $\omega-\rho$ splitting since in addition to the source considered here, this splitting will receive contributions from other sources, for example the "pure annihilation" time ordering shown in Fig. 1(a).

Our calculation has nothing to say about such "pure annihilation" contributions to OZI violation. However, we note that there are several reasons to believe that such contributions are small. In the first place, the unitarity puzzle does not apply to them so that they are not "required" to be large. In addition, to the extent that they may be characterized as proceeding through virtual glueball intermediate states [16] (which experimentally seem to have large masses), they would be suppressed. Of course, before the OZI rule can be declared to be understood, these contributions will also have to be reliably estimated.

There are a number of reasons why the full calculation leaves nearly intact the closure-approximation result that $\Delta m_\omega = \Delta m_\rho$. There is, first of all, the fact that some contributions cancel exactly even with energy denominators. Consider $\rho \to BC_1$ where B has isospin zero and C_1 has isospin one. The corresponding mode $\omega \to BC_0$, where

TABLE II. The sum leading $\Delta m_\omega - \Delta m_\rho$, to be compared with the closure approximation sum of Table I(a). The entries are in MeV. The sum of all entries is +13 MeV.

	$L=1$	$L=3$	$L=5$	$L=7$	$L=9$
$N=0$	−106	98	5	8	2
$N=1$	−35	26	−1	4	1
$N=2$	−4	10	0	2	0
$N=3$	−2	3	0	1	0
$N=4$	0	1	0	0	0

TABLE III. Mass shifts from some individual virtual decay modes. Note that ρf_J, for example, stands for the sum of the three channels ρf_0, ρf_1, and ρf_2.

Virutal decay mode	Δm_ρ (MeV)	Virtual decay mode	Δm_ω (MeV)
$\rho\to\pi\pi$	−142		
$\to\pi\omega$	−146	$\omega\to\pi\rho$	−445
$\to\eta\rho$	−63	$\to\eta\omega$	−62
$\to\eta'\rho$	−42	$\to\eta'\omega$	−41
$\to\rho\rho$	−296		
$\rho\to\pi h_1$	−81	$\omega\to\pi b_1$	−241
$\to\pi a_J$	−312		
$\to\eta b_1$	−34	$\to\eta h_1$	−34
$\to\eta' b_1$	−23	$\to\eta' h_1$	−23
$\to\rho b_1$	−183		
$\to\rho f_J$	−330	$\to\rho a_J$	−980
$\to\omega a_J$	−326	$\to\omega f_J$	−325

C_0 is an isospin zero nonet partner of C_1, has the same amplitude and energy denominator if the nonet in question is ideally mixed, so these mass shifts cancel exactly. Thus $\rho\to\eta\rho$ cancels $\omega\to\eta\omega$, $\rho\to\eta b_1$ cancels $\omega\to\eta h_1$, and $\rho\to\omega a_J$ cancels $\omega\to\omega f_J$. In other cases *pieces* of similar contributions cancel against each other even after energy denominators are in place. For example, in Table III parts of $\omega\to\pi\rho$, $\omega\to\pi b_1$, and $\omega\to\rho a_2$ cancel against $\rho\to\pi\omega$, $\rho\to\pi h_1$, and $\rho\to\rho f_2$, respectively. Thus $\omega\to\pi\rho\to\omega$ has an intrinsic transition strength which is $(\sqrt{6})^2$ times that of $\rho\to\pi\pi\to\rho$ while $\rho\to\pi\omega\to\rho$ has an intrinsic transition strength that is only $(\sqrt{2})^2$ times that of $\rho\to\pi\pi\to\rho$; only the *mismatch* of strengths contributes to $m_\omega - m_\rho$. We next note that if $2N+L$ is large, the cancellation of the dominant $l=0$ and 1 terms is maintained because the energy denominators of these terms are then approximately equal and independent of q. At smaller N and L, the mechanism mentioned in point (iv) of Sec. II is at work. We recall the argument by reconstructing it explicitly in the "magic" limit for the decays $\omega\to\rho\pi$ and $\rho\to\rho b_1$, which are parts of the (0,0,1) cancellation with (1,0,0)+(0,1,0). There, the squared matrix element of the $(l_B, l_C, l)=(0,0,1)$ $\omega\to\rho\pi$ term is the form $(q/\beta)^4\exp(-q^2/2\beta^2)$ and in the harmonic-oscillator model its energy denominator would be $-[2m+q^2/2m]$, whereas for the (1,0,0) +(0,1,0) $\rho\to\rho b_1$ term these quantities are $3(q^2/\beta^2)\exp(-q^2/2\beta^2)$ and $-[2m+\omega+q^2/2m]$. The first term peaks at $q=2\beta$, where its energy denominator is $-[2m+(2\beta^2/m)]$ and the second peaks at $q=\sqrt{2}\beta$ where its energy denominator is also $-[2m+2\beta^2/m]$, since $\omega=\beta^2/m$. This tendency of the two energy denominators to be equal at the point where their respective matrix elements have the strongest support aids the large cancellation of departures from the closure approximation. See Fig. 8. Of course, for the low-mass intermediate states where large spin splittings produce large and effectively random deviations from the closure limit, cancellations are aided by the simple fact that the momentum integral in (15) has no support at $q=0$, where the energy denominators are most different.

There is another structural reason why the energy shifts cancel so well. In the closure approximation, it is not just the entire sum over intermediate states that gives zero: one may hold fixed the spin directions of the four intermediate state quarks and sum over the remaining quantum numbers. The P-wave created pair will still have no overlap with the S-wave ρ or ω, so this restricted sum will still give zero. In other words, the closure sum can be separated into three pieces, labeled by the

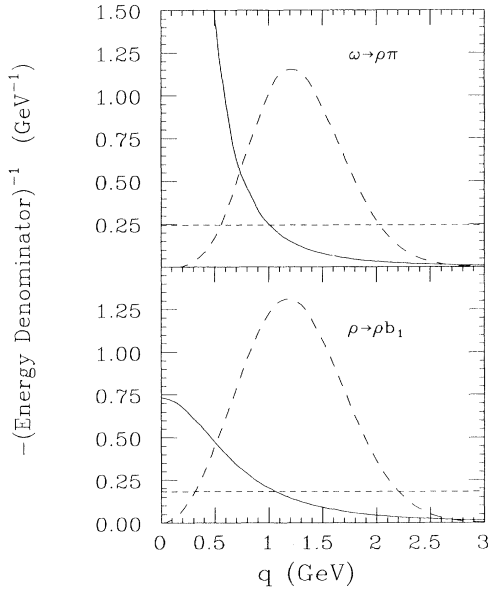

FIG. 8. For the virtual P-wave decay $\omega\to\rho\pi$ and the S-wave piece of $\rho\to\rho b_1$, we display the energy denominators (solid lines) against a background of the respective numerators (shown in arbitrary units by the long-dashed lines). The short-dashed lines are "effective energy denominators," i.e., constants which give the same energy shifts as the real energy denominators. Note that in each case the short-dashed line intersects the solid line near the peak in the numerator. The approximate equality of the two "effective energy denominators" indicates that the differences in the matrix elements for these processes tend to compensate for the differences in the energy denominators and hence to preserve the cancellations that occur in the closure limit.

TABLE IV. Sensitivity of $\Delta m_\omega - \Delta m_\rho$ to changes in β, r_c and b; the first row shows our "canonical" parameters for comparison.

β (GeV)	r_q (fm)	b (GeV^2)	$\Delta m_\omega - \Delta m_\rho$ (MeV)
0.4	0.15	0.18	+13
0.4	0.30	0.18	−33
0.3	0.15	0.18	+31
0.4	0.15	0.12	+32

total quark spin of mesons B and C, $(s_B,s_C)=(0,0),(1,0)+(0,1)$, and (1,1), and each piece is separately zero. The cancellation of the ρ and ω energy shifts is somewhat less surprising in view of this observation, since, instead of a cancellation of two large numbers, cancellations are occurring in several pairs of smaller numbers.

As a practical measure of the efficacy of the mechanisms we have described in maintaining the validity of the closure approximation, we show in Table IV the effect on the $\omega-\rho$ splitting of various changes in our model.

IV. CONCLUSIONS AND OUTLOOK

As already emphasized in the preceding, the calculation presented here was not an attempt to accurately obtain the $\omega-\rho$ mass difference (or equivalently the OZI-violating amplitude A_ω). The large cancellation which determines the contribution of virtual decay channels to A_ω makes this a very difficult task, and in addition there are other contributions to A_ω which we have not considered here. Rather, our goal was to first suggest and then substantiate a mechanism which could allow us to understand why $\Lambda_{\rm OZI}$ is so small relative to strong decay widths, and we are satisfied that we have succeeded in part in doing so.

Before even this limited task can be completed, however, much remains to be done. There are some obvious undertakings. Perhaps the first task is to understand more deeply if possible and to demonstrate explicitly in a wider range of models the resilience of the closure and spectator approximations. It is also important to explicitly calculate ω-ϕ mixing to check the validity of the SU(3) approximations made in Eqs. (1). In this system one will encounter for the first time a new potential source of OZI violation already emphasized by Lipkin: when a state is just above the threshold for a channel which could contribute to the "second-order paradox," the imaginary part of the mass matrix can receive contributions which cannot be cancelled by higher mass thresholds. Another obvious task is to extend the calculations presented here to other mesons where OZI violations are known to be small. This extension will require the use of more realistic models for the flux-tube overlap function since in general the spectator approximation will not be obeyed exactly. It is also clearly important to examine the scalar mesons where the effects of virtual decay channels can be expected to be very different. Eventually one will also wish to extend the picture of OZI violation being proposed here from the simplest case of mass mixing to general reaction processes.

ACKNOWLEDGMENTS

N.I. wishes to acknowledge the impact on the research described here of discussions over many years with Professor H. J. Lipkin of the Weizmann Institute. He is also grateful to the College of William and Mary for its support. P.G. would like to thank the Continuous Electron Beam Accelerator Facility (CEBAF) Theory Group for its hospitality and financial support during the period when this work was completed. We thank Professor O. W. Greenberg for pointing out an error in the original version of this paper. This research was supported in part by the Natural Sciences and Engineering Research Council of Canada and by the U.S. Department of Energy under Contract No. DE-AC05-84ER40150.

APPENDIX: DETERMINATION OF THE PARAMETERS OF THE MODEL

As indicated in the text, our version of the $^3P_0$ model has two adjustable parameters: the pair-creation strength γ_0, and the quark form-factor parameter r_q. In addition, the meson harmonic-oscillator wave functions are characterized by a parameter β. Here we discuss our choices of numerical values for these parameters and the sensitivity of our results to parameter variations.

Our procedure was to fix r_q, and the determine γ_0 by fitting the $^3P_0$ meson decay model to the measured $\rho\to\pi\pi$ rate. Then the rates of 26 other measured meson decays were calculated, and the goodness of fit to this sample was evaluated as a function of r_q. (See Refs. [5] and [13] for details of $^3P_0$ decay calculations, and for a tabulation of the 26 decays used in our fitting procedure. Note, however, that the r_q dependence of the decay amplitudes was calculated incorrectly in Ref. [5] so that Fig. 12 and the fourth column of Table III in that paper are in error.) The results of this fit are shown in Fig. 9. It can be seen that $r_q \approx 0.15$ fm is slightly preferred by the data, while $r_q \gtrsim 0.35$ fm is unlikely. This occurs because de-

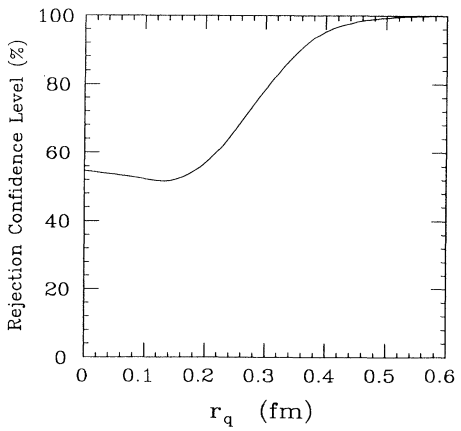

FIG. 9. Goodness of fit to meson-decay data vs the "constituent quark radius" r_q.

cays to final states with large relative momenta are fitted poorly when the pair-creation operator becomes very soft. Row 2 of Table IV shows how the $\omega-\rho$ mass difference changes when r_q is doubled from our "canonical" value of 0.15 fm to 0.30 fm.

We follow Ref. [13] in choosing 0.4 GeV as our preferred value for β. As discussed in that paper, 0.4 GeV represents for low-lying mesons an average effective β value, where the "effective β value" of a state is defined to be the β of the corresponding harmonic-oscillator wave function which reproduces that state's rms momentum (as calculated, for example, in the quark model of Ref. [14]). Row 3 of Table IV shows that our conclusions are not very sensitive to β.

Finally, though the size of the $^3P_0$ string overlap function $\exp(-b\omega^2/2)$ has not been treated as a parameter in previous applications of the flux-tube $^3P_0$ model (the size $(b/2)^{-1/2}$, where b is the QCD string tension, follows from the string-breaking picture as described in Ref. [13]), we show in row 4 of Table IV the result of changing the numerical value of b in this function.

---

*On leave from the Department of Physics, University of Toronto, Toronto, Canada M5S 1A7.

[1] S. Okubo, Phys. Lett. **5**, 1975 (1963); Phys. Rev. D **16**, 2336 (1977).

[2] G. Zweig, CERN Report No. 8419 TH 412, 1964; reprinted in *Developments in the Quark Theory of Hadrons,* edited by D. B. Lichtenberg and S. P. Rosen (Hadronic, Massachusetts, 1980).

[3] J. Iizuka, K. Okada, and O. Shito, Prog. Theor. Phys. **35**, 1061 (1965); J. Iizuka, Prog. Theor. Phys. Suppl. **37**, 38 (1966).

[4] H. J. Lipkin, Nucl. Phys. **B291**, 720, (1987); Phys. Lett. B **179**, 278 (1986); Nucl. Phys. **B244**, 147 (1984); Phys. Lett. **124B**, 509 (1983); A. Katz and H. J. Lipkin, *ibid.* **7**, 44 (1963); H. J. Lipkin, Phys. Rev. Lett. **13**, 590 (1964); **14**, 513 (1965); H. J. Lipkin and S. Meshkov, *ibid.* **14**, 680 (1965); G. Alexander, H. J. Lipkin, and F. Scheck, *ibid.* **17**, 412 (1966); H. J. Lipkin, Phys. Rep. **8C**, 173 (1973); in *New Directions in Hadronic Spectroscopy,* Proceedings of the Summer Symposium, Argonne, Illinois, 1975, edited by S. L. Kramer and E. L. Berger (Argonne National Laboratory Report No. ANL-HEP-CP-75-78, Argonne, 1975), p. 96; Phys. Lett. **60B**, 371 (1976); in *New Fields in Hadronic Physics,* Proceedings of the Eleventh Rencontre de Moriond, Flaine-Haute-Savoie, France, 1976, edited by J. Tran Tranh Van (Laboratoire de Physique Theoretique et Particules Elementaires, Universite de Paris-Sud, Orsay, France, 1976), Vol. I, p. 169; in *Understanding the Fundamental Constituents of Matter,* Proceedings of the 1976 International School of Subnuclear Physics, Erice, Italy, edited by Antonio Zichichi (European Physical Society, Geneva, 1978), p. 179; Phys. Lett. **67B**, 65 (1977); in *Deeper Pathways in High-Energy Physics,* Proceedings of the Orbis Scientiae, Fourteenth Annual Meeting, Coral Gables, Florida, 1977, edited by A. Perlmutter and L. F. Scott (Plenum, New York, 1977), p. 567; in *Prospects for Strong Interaction Physics at ISABELLE,* Proceedings of the Conference, Upton, New York, 1977, edited by D. P. Sidhu and T. L. Trueman (Brookhaven National Laboratory Report No. BNL 50701, Upton, 1977), p. 177; in *Experimental Meson Spectroscopy 1977,* Proceedings of the Fifth International Conference, Boston, Massachusetts, 1977, edited by Eberhard von Goeler and Roy Weinstein (Northeastern University Press, Boston, 1977), p. 388. For closely related work, see C. Schmid, D. M. Webber, and C. Sorensen, Nucl. Phys. **B111**, 317 (1976); E. L. Berger and C. Sorensen, Phys. Lett. **62B**, 303 (1976).

[5] P. Geiger and N. Isgur, Phys. Rev. D **41**, 1595 (1990).

[6] A. De Rújula, H. Georgi, and S. L. Glashow, Phys. Rev. D **12**, 147 (1975); H. Fritzsch and P. Minkowski, Nuovo Cimento **30A**, 393 (1975); N. Isgur, Phys. Rev. D **12**, 3770 (1975); **13**, 122 (1976).

[7] Particle Data Group, J. J. Hernández *et al.*, Phys. Lett. B **239**, 1 (1990).

[8] H. Fritzsch and J. D. Jackson, Phys. Lett. **66B**, 365 (1977); C. De La Vaissiere, Nuovo Cimento **41A**, 419 (1977); R. H. Capps, Phys. Rev. D **18**, 848 (1978); H. F. Jones and M. D. Scadron, Nucl. Phys. **B155**, 409 (1979); K. Hirata, T. Kobayashi, and Y. Takaiwa, Phys. Rev. D **18**, 236 (1978); J. F. Donoghue and H. Gomm, *ibid.* **28**, 2800 (1983).

[9] I. Cohen and H. J. Lipkin, Nucl. Phys. **B151**, 16 (1979); P. J. O'Donnell and R. H. Graham, Phys. Rev. D **19**, 284 (1979); A. T. Filipov, Yad. Fiz. **29**, 1035 (1979) [Sov. J. Nucl. Phys. **29**, 534 (1979)]; F. D. Gault and A. B. Rimmer, Z. Phys. C **8**, 353 (1981); A. B. Rimmer, Phys. Lett. **103B**, 459 (1981); E. Witten, Nucl. Phys. **B156**, 269 (1979).

[10] N. A. Tornqvist, Acta Phys. Polonica B **16**, 503 (1985), and references therein.

[11] L. Micu, Nucl. Phys. **B10**, 521 (1969); A. Le Yaouanc, L. Oliver, O. Pène, and J. C. Raynal, Phys. Rev. D **8**, 2223 (1973); **9**, 1415 (1974); **11**, 1272 (1975); M. Chaichian and R. Kogerler, Ann. Phys. (N.Y.) **124**, 61 (1980).

[12] N. Isgur and J. Paton, Phys. Rev. D **31**, 2910 (1985).

[13] R. Kokoski and N. Isgur, Phys. Rev. D **35**, 907 (1987).

[14] S. Godfrey and N. Isgur, Phys. Rev. D **32**, 189 (1985).

[15] The masses obtained by extrapolation were (in the notation m_{nl} allowed since we neglect spin-dependent effects at such high masses) $m_{15}=2.60$ GeV, $m_{23}=2.44$ GeV, $m_{24}=2.72$ GeV, $m_{31}=2.27$ GeV, $m_{32}=2.51$ GeV, $m_{33}=2.72$ GeV, $m_{40}=2.43$ GeV, $m_{41}=2.68$ GeV, and $m_{42}=2.85$ GeV. Note that we even used the nondegenerate ρ and ω masses of Ref. [14].

[16] See Donoghue and Gomm in Ref. [8] for why the virtual glueball interpretation can be misleading.